

# Bridging the COVID-19 Data and the Epidemiological Model using Time Varying Parameter SIRD Model

Cem Çakmaklı <sup>\*</sup>,<sup>1</sup> and Yasin Şimşek <sup>†</sup>,<sup>1</sup>

<sup>1</sup>*Koç University*

November 26, 2021

## Abstract

This paper extends the canonical model of epidemiology, SIRD model, to allow for time varying parameters for real-time measurement of the stance of the COVID-19 pandemic. Time variation in model parameters is captured using the generalized autoregressive score modelling structure designed for the typically daily count data related to pandemic. The resulting specification permits a flexible yet parsimonious model structure with a very low computational cost. This is especially crucial at the onset of the pandemic when the data is scarce and the uncertainty is abundant. Full sample results show that countries including US, Brazil and Russia are still not able to contain the pandemic with the US having the worst performance. Furthermore, Iran and South Korea are likely to experience the second wave of the pandemic. A real-time exercise show that the proposed structure delivers timely and precise information on the current stance of the pandemic ahead of the competitors that use rolling window. This, in turn, transforms into accurate short-term predictions of the active cases. We further modify the model to allow for unreported cases. Results suggest that the effects of the presence of these cases on the estimation results diminish towards the end of sample with the increasing number of testing.

**Keywords:** *COVID-19, SIRD, Observation driven models, Score models, Count data, time varying parameters*

**JEL Classification:** C13, C32, C51, I19

---

<sup>\*</sup>Correspondence to: Cem Çakmaklı, Koç University, Rumelifeneri Yolu 34450 Saryer Istanbul Turkey, e-mail: ccakmakli@ku.edu.tr.

<sup>†</sup>e-mail: ysimsek18@ku.edu.tr

# 1 Introduction

The outbreak of the new coronavirus, COVID-19, is one of most severe health crisis the world has encountered in last decades if not century. The spread of the virus has been at an unexpected pace since the burst of the pandemic first in Wuhan, China in early January of 2020. The World Health Organization has declared the outbreak of COVID-19 as a global pandemic in March 11 2020. Official records indicate that as of the end of June, more than 10 million people are infected with a total death toll approaching to half a million.

Anticipating the devastating humanitarian and economic effects of the COVID-19, countries have taken various measures to contain the pandemic. A variety of measures have been imposed ranging from complete lockdown, essentially freezing the flow of life for an uncertain period, to partial lockdown implying a partial closure to the daily routines for the protection of the most vulnerable in the population. On the contrary, some countries including Sweden, England and Netherlands were reluctant to consider any measures at first at the onset of the outbreak but rapidly switch to impose lockdown measures. Recently, a vast majority of countries has launched the process for normalization confronting economic pressures. The decision of imposing and/or relaxation of these various sorts of measures and evaluating the outcome of these actions evidently rely on efficiently monitoring the course of the pandemic. Therefore, epidemiological models for estimating, and perhaps even more crucially for predicting the trajectory of pandemic come to the forefront. However, if these measures indeed turn out to be effective and changing the natural course of the pandemic, then this implies that the parameters of the epidemiological models alter to comply this changing trajectory. This is the departure point of this paper. Specifically, we develop a simple and statistically coherent model that allows for time variation of the parameters of the conventional workhorse epidemiological model.

We start our analysis by confronting a simple version of the workhorse epidemiological model with the actual data. From the perspective of econometrics, we specify a count process for modeling the course of the COVID-19 pandemic for a selected set of countries based on the SIRD model. The SIRD model identifies the four states of the pandemic as Susceptible, Infected, Recovered and Death and it depicts the evolution of these states depending on the total number of infected individuals, see Kermack and McKendrick (1927); Allen (2008). It is the contestation of these forces, i.e. the parameters governing

the rates of infection and resolution (in the form of recovery or death) that determines the course of pandemic. Therefore, we extend the econometric model by allowing for time variation in the structural parameters resorting to the Generalized Autoregressive Score (GAS) modeling framework which is a class of observation-driven models. The proposed model permits a flexible yet feasible framework that can track the evolution of structural parameters quite timely and accurately. One important aspect of our specification is its relatively low computational cost, which might be crucial especially at the beginning of the pandemic when the data is scarce and the uncertainty is overwhelming.

We construct a set of selected countries that so far have experienced different courses of pandemic to demonstrate the efficacy of the proposed framework. These include countries that can mitigate the pandemic but with differential momentum, countries where the pandemic starts relatively late and countries that experience a second wave of pandemic. This provides us a testing ground with a wide variety of patterns to examine the potential of the proposed model. Our results indicate that for a majority of countries the structural parameters alter over time. The rate of infection typically starts at a high level at the onset of the pandemic and but it decreases at distinct paces depending on the success of the country in containing the transmission of the virus. On the contrary, the recovery rate starts at a low level and gets stabilized after an increase from these low values reflecting the performance of health systems in handling the active cases. As a result, the reproduction rates, computed as the ratio of the infection rate to the recovery and mortality rates, start at high levels often exceeding the value 5, but diminish at differential rates. Two crucial findings emerge from the outcomes of the proposed model with time varying parameters. First, US, Russia and Brazil still cannot tackle with the (first wave of) pandemic as the reproduction rates have not fallen below the critical value of 1. Second, Iran and South Korea seem to experience the second wave of the pandemic.

We further examine the real-time performance of the models. It is crucial for the models to indicate the stance of the pandemic in real-time and to provide accurate and timely predictions at least in the short-run. A real-time estimation and forecasting exercise starting from April show that the proposed model with time varying parameters indeed provide timely information on the current stance of the pandemic ahead of the competing models. Moreover, it also provides superior forecasting performance up to 1 week ahead, especially for those countries who are currently experiencing the second wave of

the pandemic. Finally, we extend the model for including the cases that are undocumented (as these infected individuals do not show symptoms) using the strategy in Grewelle and De Leo (2020). While inclusion of those leads to large discrepancies in parameters compared to initial findings especially at the onset of the pandemic, parameter values converge to similar values towards the end of May as the cumulative figures mount.

The literature on estimating the SIRD model (with fixed parameters) and variants to evaluate the current stance of the COVID-19 pandemic has exploded since the outbreak of the pandemic. Relatively earlier analysis include Read et al. (2020) and Lourenco et al. (2020) who estimate a SIRD based model with the data from China for the former and for the UK and Italy for the latter using a likelihood based inference strategy. Wu et al. (2020) blend data related to COVID-19 for China with mobility data and estimate the epidemiological model using Bayesian inference to predict the spread of the virus domestically and internationally. Li et al. (2020) conduct a similar analysis employing a modified SIR model together with a network structure and mobility data to uncover the size of the undocumented cases, see also Hortaçsu et al. (2020). Zhang et al. (2020) extend the standard SIR model with many additional compartments and estimate a part of parameters using Bayesian inference.

Several factors might lead to time variation in the parameters of the epidemiological model regarding to the course of pandemic. On the one hand, the lockdown measures taken by the policy makers are intended to isolate the infected from the susceptible individuals. Therefore, the parameter governing the rate of infection which is simply the average number of contacts of a person is likely to alter with the conduct of lockdown, see for example Hale et al. (2020). On the other hand, advancements in the fight against COVID-19 including the recovery of drugs that could effectively mitigate the course of the disease, the installment or the lack of the medical equipment such as ventilators might alter the rate of recovery or in other words the duration of the state of being infected, see for example Greenhalgh and Day (2017) on time variation in recovery rates. Accordingly, Anastassopoulou et al. (2020) use a least squares based approach on a rolling window of daily observations and document the time variation of parameters in the SIRD based model using Chinese data. Tan and Chen (2020) also employ a similar but more articulated rolling window strategy to capture the time variation in the model parameters. Other frameworks with time varying model parameters almost exclusively allow for the

time variation only in the infection rate. An application prior to COVID-19 outbreak includes, for example, Xu et al. (2016) among others, who utilize a Gaussian process prior for the incidence rate involving the rate of infection using a Bayesian nonparametric structure. In the context of COVID-19 pandemic, Kucharski et al. (2020) estimate a modified SIR model using a parameter driven model framework allowing the infection rate to follow a geometric random walk with the remaining parameters kept as constant, see Marioli et al. (2020) for a similar approach. Similarly, Yang et al. (2020) and Fernandez-Villaverde and Jones (2020) allow for time variation in the rate of infection keeping the remaining parameters constant.

In this paper, we propose an alternative modeling strategy to capture the time variation in the full set of structural parameters of the SIRD model. On the one hand, our modeling framework is statistically consistent with the typical count data structure related to pandemic unlike the models that either employ least squares based inference or likelihood based inference using Gaussian distribution, e.g. Kalman filter. On the other hand, our framework is computationally inexpensive unlike the models that are statistically consistent but employing particle filter type of methods for inference which are computationally quite costly. This might be crucial especially at the onset of the pandemic when the data is scarce and uncertainty about the course of pandemic is abounding. Our framework belongs to the class of observation driven models and specifically to the class of Generalized Autoregressive Score Models (henceforth GAS Models) proposed by Creal et al. (2013). GAS models involve many of the celebrated econometric models including Generalized Autoregressive Heteroskedasticity (GARCH) model and various variants as a special case, and thus, they proved to be useful in both model fitting as well as prediction. Koopman et al. (2016) provides a comprehensive analysis on predictive power of these models compared to parameter driven models in many settings including models with count data.

Independent of the analysis of COVID-19 pandemic, observation-driven models for count data are considered in many different cases. Davis et al. (2003) provides a comprehensive analysis on observation driven models with a focus on data with (conditional) Poisson distributions. Ferland et al. (2006) derives an integer-valued analogue of the GARCH model (IN-GARCH) using Poisson distribution instead of Gaussian distribution. Fokianos et al. (2009) considers the Poisson autoregression of linear as well as nonlinear form including IN-GARCH model as a specific case. Chen and Lee (2016) extend the

Poisson autoregression to allow for smooth regime switches in parameters. Our framework naturally extends these approaches to the epidemiological model framework for each of the compartments of the SIRD model essentially using a multivariate structure.

The remainder of the paper is organized as follows. In Section 2 we describe the canonical SIRD model and introduce the SIRD model with time varying parameters with full details provided in the Appendix. In this section, we discuss the estimation results using full sample data from various countries. In Section 3, we discuss the real-time performance of our model framework in capturing the current stance of the pandemic as well as in short-term forecasting compared to frequently used competitors. In Section 4, we extend the model to account for infected individuals who are not diagnosed and therefore not included in the sample. Finally, we conclude in Section 5.

## 2 The canonical model of pandemic, SIRD model

We start our analysis with the epidemiological model denoted as the SIRD model of Kermack and McKendrick (1927), which is the acronym of Susceptible, Infected, Recovered and Death individuals. Specifically, the SIRD model categorizes the population into these four classes of individuals representing four distinct states of the pandemic as Susceptible ( $S_t$ ), Infected ( $I_t$ ) and Recovered ( $R_t$ ) and Death ( $D_t$ ) in period  $t$ . The susceptible group does not yet have immunity to disease, and individuals in this group have the possibility of getting infected. The recovered group, on the other hand, consists of individuals who are immune to the disease, and finally  $D_t$  represents individuals that have succumbed to the disease. The Susceptible-Infected-Recovered-Death (SIRD) model builds on the principle that fraction of the infected individuals in the population,  $\frac{I_{t-1}}{N}$ , can transmit the disease to susceptible ones  $S_{t-1}$  with an (structural) infection rate of  $\beta$  by assuming a quadratic matching in the spirit of gravity law, see Acemoglu et al. (2020) for details on alternative matching structures. Therefore, the number of newly infected individuals in the current period is  $\beta S_{t-1} \frac{I_{t-1}}{N}$ . The newly infected individuals, i.e. confirmed cases, should be deducted from the susceptible individuals in the current period. Meanwhile, in each period, a fraction  $\gamma$  of the infected people recovers from the disease, which in turn reduces the number of actively infected individuals. Similarly, a fraction  $\nu$  of the infected people have succumbed to the disease further reducing the number of actively infected individuals.

Hence, a fraction  $\gamma + \nu$  of the infections are ‘resolved’ in total. This leads to the following sets of equations:

$$\begin{aligned}\Delta S_t &= -\beta S_{t-1} \frac{I_{t-1}}{N} \\ \Delta R_t &= \gamma I_{t-1} \\ \Delta D_t &= \nu I_{t-1} \\ \Delta I_t &= \beta S_{t-1} \frac{I_{t-1}}{N} - (\gamma + \nu) I_{t-1}\end{aligned}\tag{1}$$

Note that the last equation defines the law of motion for the number of infected individuals and it is the outcome of the first three equations as  $\Delta S_t + \Delta R_t + \Delta I_t + \Delta D_t = 0$  holds at any given time, assuming that the size of the population remains constant.<sup>1</sup>

## 2.1 Estimation of the SIRD model with fixed parameters

The parameters of interest are the structural parameters  $\beta$ ,  $\gamma$  and  $\nu$  that provide information on the transmission and resolution rates of the COVID-19 pandemic, respectively. A central metric which characterizes the course of the pandemic is the reproduction number,  $R_0$ . The reproduction number refers to the speed of the diffusion which can be computed by the ratio of newly confirmed cases, denoted as  $\Delta C_t$ ,<sup>2</sup> to the resolved cases, that is  $\Delta C_t / (\Delta R_t + \Delta D_t)$ . Therefore, it serves as a threshold parameter of many epidemiological models for disease extinction or spread. Considering the fact that  $S_t/N \approx 1$ ,  $R_{0,t}$  can be approximated by  $\beta/(\gamma + \nu)$  in (1) and it holds exactly when  $t = 0$ , referred as the basic reproduction rate  $R_0$ . In this sense, a value of  $R_0$  being less than unity indicates that the pandemic is contained and if it exceeds unity, this implies that the spread of the pandemic continues. Inference on  $\beta$ ,  $\gamma$  and  $\nu$  and thereby inference on  $R_0$  enables us to track the trajectory of the pandemic. Our main motivation for employing the model from the econometrics point of view is to conform this canonical epidemiological model with the actual datasets and pinpoint the stance of the pandemic timely. For that purpose, we first discretize (1) as the typical COVID-19 dataset involves daily observations on the counts of individuals belonging to these states of health. Motivated by this, we specify a counting process for the states using the Poisson distribution with conditional arrivals implying a nonhomogenous Poisson process for all the counts see for example Allen (2008); Yan (2008); Rizioi et al. (2018) for earlier examples and Li et al. (2020) in the COVID-19

---

<sup>1</sup>In fact, the number of deaths reduces the total population. We assume that the total number of deaths is negligible compared to the population for the sake of tractability of the resulting SIRD model.

<sup>2</sup> $\Delta C_t$  is identical to  $-\Delta S_t$ , i.e. the deduction in the number of susceptible individuals.

context for a similar approach. This leads to the following specification for the stochastic evolution of counts of these states

$$\begin{aligned}
\Delta C_t | \Omega_{t-1} &\sim \text{Poisson}(\beta \frac{S_{t-1}}{N} I_{t-1}) \\
\Delta R_t | \Omega_{t-1} &\sim \text{Poisson}(\gamma I_{t-1}) \\
\Delta D_t | \Omega_{t-1} &\sim \text{Poisson}(\nu I_{t-1}) \\
\Delta I_t &= \Delta C_t - \Delta R_t - \Delta D_t
\end{aligned} \tag{2}$$

where  $\Omega_t$  stands for information set that is available up to time  $t$ . We assume that  $\Delta C_t$ ,  $\Delta R_t$  and  $\delta D_t$  are independent conditional on  $\Omega_{t-1}$ . The resulting distribution for the active number of infections,  $I_t$ , is a Skellam distribution (conditional on  $\Omega_{t-1}$ ) with the mean  $\pi I_{t-1} = (1 + \beta(R_0^{-1} - 1))I_{t-1}$  and the variance as  $\beta(R_0^{-1} + 1)I_{t-1}$ , where we use the identity in the last equation together with the definition of  $R_0$ . Therefore, stationarity of the resulting process depends on whether  $R_0 < 1$  or  $R_0 \geq 1$ , i.e. whether the pandemic is taken under control or not. While moments conditional on  $I_{t-1}$  is identical due to Poisson distribution, the first and second moments diverge when we consider the unconditional moments. In this case,

$$\begin{aligned}
E[I_t] &= \pi^t I_0 \\
\text{Var}(I_t) &= \beta(1 + R_0^{-1}) \frac{\pi^{t-1}(1-\pi^t)}{1-\pi} I_0,
\end{aligned} \tag{3}$$

where we assume that the initial condition,  $I_0$ , is known. If the initial condition is considered as a parameter to be estimated then the variance is further amplified with a factor in terms of the variance of the initial condition. Accordingly, the unconditional moments of the states of the pandemic are linear functions of these unconditional moments of  $I_t$ . We refer to Appendix B.1 for details.

We conduct Bayesian inference using the likelihood implied by (2) together with non-informative priors for estimating the model parameters. Specifically, for all the models, we use independent Metropolis-Hastings algorithm using Normal distribution around the posterior mode and Hessian as the candidate density, see Robert and Casella (2013) for details. We use the data of selected set of countries starting from the early days of pandemic until the end of second week of June. For each country, we use the day when the number of confirmed cases exceeds 1000 as the starting point of the sample. We display the dataset in Table 1.

[Insert Table 1 about here]

These countries exhibit extensive heterogeneity in terms of their experience related to pandemic. Some countries in this set impose strict measures of full lockdown and successful policies of testing and tracing promptly at the onset of the pandemic including South Korea, while other countries including Italy has imposed these immense measures after a certain threshold regarding the number of infected individuals. Some others opt for imposing mixed strategies involving partial lockdowns and voluntary quarantine such as Turkey and US. We also include other interesting cases including Brazil and Russia who are going through differential phases of the pandemic. Finally, Iran experiences a second wave of the pandemic, though South Korea seems to start a similar pattern, albeit much milder. Hence, this relatively rich and heterogeneous dataset involving countries with all sorts of pandemic experience enables us to examine the success of the econometric model in tracking the changes in the structural parameters as a response to this policy implementations. The estimates of the model parameters are displayed in Table 2.

[Insert Table 2 about here]

We first focus on the basic reproduction rate,  $R_0$  as displayed in the last column of Table 2. For all countries but South Korea  $R_0$  exceeds the threshold of 1 and for some it also exceeds 2. Apparently, when the full sample of several days is taken into account, estimation results show that in almost none of the countries in our sample the pandemic could be taken under control. For Brazil, Russia and US who experience relatively prolonged earlier phases of the pandemic we estimate an  $R_0$  that is very close to 2 or that exceeds 2 departing from the rest of the countries in the sample. This is due to the almost exceptional low recovery rate for the case of US and high rate of infection for Brazil. Indeed, two groups come into view considering the infection rate. Brazil and Iran constitute the group with high infection rate departing from the remaining countries. A similar grouping appears also for the mortality rate. In this case Italy joins to the group of high mortality rate together with Brazil and Iran.

The estimation results in Table 2 rely on the SIRD model with fixed parameters as demonstrated in (2). While, as of the second week of June it is widely accepted that the pandemic is taken under control in countries including South Korea, we still obtain an  $R_0$  very close to 1. This might be due to rapid pace of infectiousness, captured by  $\beta$ , at the

onset of the pandemic which is brought under control due to rapidly imposed measures. Moreover, increasing knowledge about the SARS-Cov-2 virus, availability of the medical care facilities such as ICU's and more effective treatment of the infection potentially lead to changes in the recovery rate  $\gamma$  and the mortality rate  $\nu$ . Therefore, it might be crucial to model this time variation efficiently in a data scarce environment allowing for estimation at the onset of the pandemic as well.

## 2.2 SIRD model with time varying parameters - TVP-SIRD

In this section we put forward the SIRD model with time varying parameters. For modeling the time variation we use the framework of Generalized Autoregressive Score model (GAS hereafter) which encompasses a wide range of celebrated models in econometrics, including Generalized Autoregressive Conditional Heteroscedasticity model (GARCH) and its variants. Briefly, the GAS model relies on the intuitive principle of modeling the time variation in key parameters in an autoregressive manner which evolves in the direction implied by the score function and thereby improving the (local) likelihood, see Creal et al. (2013) for a detailed analysis of the GAS model. As in the case of the GARCH model, it effectively captures the time dependence in long lags in a parsimonious yet quite flexible structure. Perhaps more importantly, since it admits a recursive deterministic structure the resulting data driven time variation in parameters is computationally inexpensive to estimate. This might be crucial given that these flexible models are evaluated throughout the course of the pandemic when data is often scarce especially at the onset of it. Consider the SIRD model with time varying parameters as  $\beta_t$ ,  $\gamma_t$  and  $\nu_t$ . We first transform these parameters into logarithmic terms to ensure positivity of these parameters and thereby the positivity of the predicted counts every time period. Let the parameter with a tilde denote the logarithmic transformations as  $\tilde{\beta}_t = \ln(\beta_t)$ ,  $\tilde{\gamma}_t = \ln(\gamma_t)$  and  $\tilde{\nu}_t = \ln(\nu_t)$ . The

resulting Time Varying Paramaters - SIRD (TVP-SIRD) model is as follows

$$\begin{aligned}
\Delta C_t | \Omega_{t-1} &\sim \text{Poisson}(\beta_t \frac{S_{t-1}}{N} I_{t-1}) \\
\Delta R_t | \Omega_{t-1} &\sim \text{Poisson}(\gamma_t I_{t-1}) \\
\Delta D_t | \Omega_{t-1} &\sim \text{Poisson}(\nu_t I_{t-1}) \\
\tilde{\beta}_t &= \alpha_0 + \alpha_1 \tilde{\beta}_{t-1} + \alpha_2 s_{1,t} \\
\tilde{\gamma}_t &= \phi_0 + \phi_1 \tilde{\gamma}_{t-1} + \phi_2 s_{2,t} \\
\tilde{\nu}_t &= \psi_0 + \psi_1 \tilde{\nu}_{t-1} + \psi_2 s_{3,t} \\
\Delta I_t &= \Delta C_t - \Delta R_t - \Delta D_t
\end{aligned} \tag{4}$$

where  $s_{1,t}$ ,  $s_{2,t}$  and  $s_{3,t}$  are the (scaled) score functions of the joint likelihood. Since the likelihood function of the SIRD model is constituted by the (conditionally) independent Poisson processes, each score function is derived using the corresponding compartment. Specifically, let  $\nabla_{1,t} = \frac{\partial L(\Delta C_t; \tilde{\beta}_t)}{\partial \tilde{\beta}_t}$ ,  $\nabla_{2,t} = \frac{\partial L(\Delta R_t; \tilde{\gamma}_t)}{\partial \tilde{\gamma}_t}$  and  $\nabla_{3,t} = \frac{\partial L(\Delta D_t; \tilde{\nu}_t)}{\partial \tilde{\nu}_t}$  denote the score functions of the likelihood function for period  $t$  observation. We specify  $s_{i,t}$  such that the score functions are scaled by their variance as  $s_{i,t} = \frac{\nabla_{i,t}}{\text{Var}(\nabla_{i,t})}$  for  $i = 1, 2, 3$ .<sup>3</sup> In the specific case of SIRD model, this modeling strategy leads to the following specification for the (scaled score functions) in terms of the logarithmic link function

$$\begin{aligned}
s_{1,t} &= \frac{\Delta C_{t-1} - \lambda_{1,t-1}}{\lambda_{1,t-1}} \\
s_{2,t} &= \frac{\Delta R_{t-1} - \lambda_{2,t-1}}{\lambda_{2,t-1}} \\
s_{3,t} &= \frac{\Delta D_{t-1} - \lambda_{3,t-1}}{\lambda_{3,t-1}}
\end{aligned} \tag{5}$$

where  $\lambda_{1,t} = \beta_t \frac{I_{t-1} S_{t-1}}{N}$ ,  $\lambda_{2,t} = \gamma_t I_{t-1}$  and  $\lambda_{3,t} = \nu_t I_{t-1}$ . The resulting specification implies an intuitive updating rule in the sense that the parameters (in logarithmic form) are updated using a combination of recent parameter value and recent percentage deviation from the mean. We refer to Appendix A for the details on derivation of (5). The specification in (4) leads to quite rich dynamics both in terms of mean and the variance of the resulting process. This enables us to capture the evolution of the pandemic accurately which is reflected as timely and prompt response of the parameters to the changes in the data, i.e. in the states of the pandemic. We refer to Appendix B.2 for the details on the properties

---

<sup>3</sup>Alternative approaches for scaling the score function include the standard deviation rather than the variance and using score function without scaling. Our experience on this experimentation is that using the variance as the scaling function leads to smoother and more robust evolution of model parameters over time.

of the process described in (4).

An appealing feature of the TVP-SIRD model is that it encompasses the SIRD model with fixed parameters. For example, when  $\alpha_1 = 1$  together with  $\alpha_0$  and  $\alpha_2$  to be zero, then the rate of infection,  $\beta_t$ , remains fixed over the course of pandemic. This would indicate that the lockdown measures are proved to be ineffective as it does not lead to a systematic change in the infection rate. Similar reasoning also applies to  $\gamma_t$  and  $\nu_t$ . Therefore, it provides a solid framework for statistically testing the efficiency of measures for taking the pandemic under control. We display the estimates of the underlying parameters governing (logarithms of)  $\beta_t$ ,  $\gamma_t$  and  $\nu_t$  in Table 3.

[Insert Table 3 about here]

The parameter estimates in Table 3 indicate that the structural parameters governing the diffusion of the infection exhibit time varying behaviour. For all the countries, the 95% credible intervals for the posterior joint distribution exclude the set of  $\alpha_0 = \alpha_2 = 0$  and  $\alpha_1 = 1$  implying that  $\beta_t$  indeed varies over time. The same conclusion also applies for the recovery rate  $\gamma_t$  and mortality rate  $\nu_t$  which is considered as constant parameters in vast majority of studies.

We display the evolution of the underlying structural parameters,  $\beta_t$ ,  $\gamma_t$ ,  $\nu_t$  and the resulting  $R_{0,t}$  over time in Figure 1.

[Insert Figure 1 about here]

Figure 1 reveals interesting patterns for the underlying parameters of the TVP-SIRD model when applied to the real datasets. First, considering  $\beta_t$ , which is the rate of infection, for Italy, Russia, Turkey and US, we observe a decreasing pattern, which seems to be stabilized afterwards. It seems that the full lockdown measures imposed by these countries have weakened the transmission of the virus throughout the society. Still, we observe a mild increase for Turkey reflecting the outcome of the normalization process. On the other hand, limited reaction to the virus in Brazil leads to fluctuations in the rate of infections which exhibits a weakly decreasing trend only starting from the end of April. Iran and South Korea exhibit an alarming pattern in the sense that while the rate of infection had landed at very low levels compared to initial values, starting with the first of week of May, we observe a take off again hinting a potential second wave of the pandemic. The results show that the dynamic structure of the flexible modeling strategy could capture many

types of pattern of the infection rate affected by the containment measures imposed by the countries.

The recovery rate seems to have less variation for a majority of countries, which usually starts with low levels as still the first wave of recoveries are limited and then getting stabilized around some fixed values. Turkey seems to be an exception with an increasing rate of recovery towards the end of April first and then at the end of May. This high rate of recovery coincides perfectly with the days right after the peak of active cases at the end of the third week of April. We also note that the uncertainty around these values also rises as a result of this rapid change. For Italy and Russia the improvement in the recovery rate is quite gradual approaching to a stable and high level only towards the last week of May.

When we consider the mortality rate, an interesting structure emerges. For all countries with the exception of South Korea the value of mortality rate is smoothly stabilized around a fixed value. While this fixed value is 0.001 for a majority of countries, it is lower for South Korea and larger for Brazil and Iran reflecting the varying capability of the health systems of these countries in coping with the pandemic. For South Korea the mortality rate of the pandemic is quite low and the seemingly volatile nature of the mortality rate might be due to these minuscule rates prone to fluctuations over time.

The course of the reproduction rate,  $R_{0,t}$  is of central importance for tracing the efficacy of the containment efforts of the pandemic. The last column of the Figure 1 displays these and we discuss our findings country by country. For Brazil, although the reproduction rate has decreased from record high levels to values around 2, it is still larger than 1. Even more crucially, the drop from 2 to values just above 1 at the beginning of June is due to sudden increase in the rate of recovery rather than a decrease in the infection rate. For Italy, the reproduction rate has fallen below the value of 1 at the beginning of May and remained there since then. Therefore, Italy seems to take the pandemic successfully under control. For Iran, the reproduction rate fell below 1 as early as mid April but it has exceeded this critical threshold starting from the second week of May and still remains above 1. As discussed earlier, this is due to the increasing infection rate, to a large extent, reflecting the potential threat of the second wave. A similar pattern is also observed for South Korea with the reproduction rate exceeded the threshold of 1 as of June. For US and Russia, while the reproduction rate has been stabilized, it does that above 1 where for Russia it is close to 1 and for US it is around the value of 2. Hence, for these countries

the pandemic is far from being contained and it continues to diffuse rapidly. Finally, for Turkey the pandemic is contained as of first week of May but the increasing pattern of the reproduction rate after May leads it to wander around values just below 1 with the beginning of normalization process similar to other countries. Considering the cases of Iran and South Korea, it might easily cross the threshold especially given the fact that the rate of infection exhibits an increasing tendency starting from the first week of June.

### 3 Real-time performance of the models

The results in the previous section display our findings based on the estimates using full sample dataset as of the end of second week of June. These results indicate that our flexible modelling structure can accommodate various forms of parameter changes reflecting the course of pandemic. However, exploring the real-time performance of the model would uncover whether this additional flexibility brought by the time varying parameters could provide timely and accurate information on the real-time stance of the pandemic. Therefore, we provide the estimates of the model parameters in real-time using the model with fixed parameters and using the model with time varying parameters. We use a moving window for performing the estimations of the SIRD model with fixed parameters as the evidence in the previous sections show that the values at the onset of the pandemic could drive the findings intensively. Specifically, using the dataset from  $t-M, t-M+1, \dots, t$ , we estimate the SIRD model and the resulting parameter estimates are those for the period  $t$ , and we repeat the process by adding one more observation (and dropping one observation at the beginning of the sample) recursively. We consider three cases by setting  $M = 10, 20$  and  $30$ , i.e. starting from ten days of data up to one month of data. For the TVP-SIRD model we use the expanding window at hand up to time period  $t$  as the parameters in this case are time varying. We display the evolution of the structural parameters,  $\beta_t, \gamma_t, \nu_t$  and the resulting  $R_{0,t}$  over time in Figure 2.

[Insert Figure 2 about here]

When we consider the rolling window estimates using the SIRD model with fixed parameters, we observe that there is a trade-off between the speed of reaction to the evolution of pandemic and the window size as expected. When the window size is taken as 30 days the parameters evolve quite smoothly but cannot react to the rapid changes promptly. On

the contrary, when 10 days of window size is used parameters adjust to the new conditions more quickly. When we focus on the time varying parameters SIRD model, we observe that the parameters can accommodate to the newly changing conditions swiftly, ahead of the SIRD model with fixed parameters regardless of the window size. In addition, they can also react to the abrupt changes in the data. Specifically, parameter estimates obtained by the TVP model is leading the estimates of the fixed parameter model with 10 days of window size by almost 2 weeks ahead. This lead time increases when we consider wider rolling window sizes. While the lead time is larger for the first half of the sample, it decreases over the course of pandemic, when the pandemic is stabilized and thus the variation in parameters are limited. This indicates that the TVP model is most useful when there are abrupt changes in the pattern of the data and the uncertainty about the course of pandemic is at highest level. To give a concrete example, we consider Brazil. In this case, the relatively mild increases in the number of active cases after 10<sup>th</sup> of April is instantly reflected to the rate of infection with the TVP model whereas this process takes much longer for the SIRD model with 10 days of window size for estimation. Considering the recovery rate, the jump in the number of recoveries in April 14 is instantly reflected to the recovery rate with the release of first set of recoveries.<sup>4</sup> For the SIRD model with 10 days of window size in inference, this process takes almost 2 weeks to reflect the changes in the numbers. As a combination of these two forces, the reproduction rate immediately fell to the levels around 1 in mid April, which bounced back again to values around 2 in about two weeks. Considering the SIRD model with 10 days of window size, the reproduction rate decreased to values around 1 around April 23<sup>rd</sup> and returned back to the values around 2 with around one week of lag. Considering the severity of the pandemic these lead times might be crucial in comprehending the current stance of the pandemic. Here we do not discuss the results with 20 and 30 days of rolling window size for the fixed parameter SIRD model as these perform worse than the model with 10 days of window size used for inference. Finally, we explore whether this capability of the TVP-SIRD model in reflecting the stance of the pandemic in a timely manner indeed proved to be useful in forecasting the number of active cases. This would also indicate whether the TVP-SIRD model indeed reflects the current stance of the pandemic in a timely but accurate manner. We therefore perform a real-time forecasting exercise where using our recursive estima-

---

<sup>4</sup>Here, we do not take a stance on the quality of the official statistics as all competing models are estimated using the same data.

tions of the models in (2) and (4) based on the information available in time period  $t$ , we perform  $h = 1, 2, \dots, 7$ -day ahead predictions of active cases, i.e.  $I_{t+h}$ . We use the first one third of the full sample as the estimation sample and we expand the window by adding one more observation and repeat the procedure. This roughly provides us at least 40 days of evaluation period for each country. We display the results involving RMSFEs of the competing models relative to TVP-SIRD model in Table 4.

[Insert Table 4 about here]

Table 4 reveals that the TVP-SIRD model outperforms the SIRD models estimated using an expanding window (EW) or using a rolling window with 10, 20 or 30 days of observations in almost all of the considered cases. First, models estimated using an expanding window or rolling windows with more than 10 days of observations perform inferior relative to the TVP-SIRD model and the SIRD model using 10 days of observations in the sense that the relative RMSFE increases monotonically with the use of more data. The closest competitor to the TVP-SIRD model is the SIRD model using 10 days of rolling window (RW-10). In this case, for 1-day ahead predictions of active cases, TVP-SIRD model provides much better predictions than the RW-10 with relative RMSFEs ranging from 1.26 for South Korea up to the value as large as 2.22 for Iran and Turkey. However, for all the models the forecasting performance deteriorates with the increasing prediction horizon. Therefore, the relative RMSFEs of the models monotonically approaches to values close to 1 for a majority of models. Still, for all countries with some exceptions the TVP-SIRD model outperforms all competing models for all horizons. For Italy and Russia, the SIRD model using 10 days of rolling window performs slightly better than the TVP-SIRD model with the relative RMSFE getting smaller as the forecast horizon increases. For Turkey and US, this outperformance of the RW-10 model starts with the 4- and 5-day forecast horizon. An interesting finding is on South Korea and Iran. In these cases, where these countries presumably go through the second wave of the pandemic, TVP-SIRD model evidently surpasses all competing models reflecting the ability of the flexible structure to accommodate the changing behavior of the pandemic rapidly.

## 4 Accounting for sample selection

A key underlying assumption of the model specification in previous sections is that the variables of the infected, recovered and succumbed individuals represent the aggregate numbers in the society. However, one of the stylized facts related to COVID-19 pandemic is the presence of the infected individuals who do not show any symptoms, denoted as asymptomatic. This complicates the analysis by leading to a selection bias in econometric inference among other factors, see Manski and Molinari (2020). The underlying reason for this bias is that only the patients who show symptoms can be detected as those are the ones who comply for the tests. These exclude a portion of the infected cases which plagues econometric inference. In this section, we provide results on the total number of individuals based on explicit assumptions on the model structure to capture asymptomatic infected individuals. Let  $I_t^*$  be the number of infected individuals involving both asymptomatic and symptomatic cases. Similarly, let  $S_t^*$ ,  $R_t^*$  and  $D_t^*$  denote the total number of susceptible, recovered and dead individuals, respectively. Throughout the analysis, we use the following assumptions,

**Assumption 1** *The total number of individuals in the state of ‘infected’ that are symptomatic constitutes a  $1 - \delta_t$  fraction of the total number of individuals in the state of ‘infected’, i.e.  $I_t = I_t^*(1 - \delta_t)$ ,*

**Assumption 2** *The total number of recovered individuals that were infected with symptoms constitutes a  $1 - \delta_t$  fraction of the total number of individuals in the state of ‘recovered’, i.e.  $R_t = R_t^*(1 - \delta_t)$ ,*

**Assumption 3** *The infected individuals that are asymptomatic always recover, and thus, they do not switch to the state of ‘death’, i.e.  $D_t = D_t^*$ .*

The second assumption implies that the recovery process for the infected individuals with and without symptoms are identical. This assumption is obviously subject to doubt, however, it saves us an extra parameter to calibrate. These assumptions serve as a rough approximation to the entire sample without deep epidemiological insight and therefore the estimation outputs should be taken with caution. Using these assumptions, the TVP-SIRD

model in terms of the total numbers can be written as

$$\begin{aligned}
\Delta C_t^* | \Omega_{t-1} &\sim \text{Poisson}(\beta_t \frac{S_{t-1}^*}{N} I_{t-1}^*) \\
\Delta R_t^* | \Omega_{t-1} &\sim \text{Poisson}(\gamma_t I_{t-1}^*) \\
\Delta D_t | \Omega_{t-1} &\sim \text{Poisson}(\nu_t I_{t-1}^*) \\
\tilde{\beta}_t &= \alpha_0 + \alpha_1 \tilde{\beta}_{t-1} + \alpha_2 s_{1,t} \\
\tilde{\gamma}_t &= \phi_0 + \phi_1 \tilde{\gamma}_{t-1} + \phi_2 s_{2,t} \\
\tilde{\nu}_t &= \psi_0 + \psi_1 \tilde{\nu}_{t-1} + \psi_2 s_{3,t} \\
\Delta C_t^* = -\Delta S_t^* &= \Delta I_t^* + \Delta R_t^* + \Delta D_t
\end{aligned} \tag{6}$$

where  $\Delta I_t^* = \frac{\Delta I_t}{(1-\delta_t)}$  and  $\Delta R_t^* = \frac{\Delta R_t}{(1-\delta_t)}$ . The key observation in these new set of equations is that the observed number of deaths are identical to the total number if the third assumption indeed holds. This, in turn, prevents the number of individuals who are susceptible to be computed as a fraction of  $1/(1-\delta_t)$  as the final equation suggests. Therefore, the evolution of the structural parameters differs from the counterpart in the previous cases, where observed data is assumed to represent the full sample. While this source of variation might suffice for the identification of the  $\delta_t$  parameter, we note that the number of deaths constitutes only a minuscule fraction of the total number of susceptible individuals. To enhance the identification of  $\delta_t$  we exploit the information in the total number of testing following Grewelle and De Leo (2020). Briefly, the underlying idea stems from the fact that the detection of the infections including the asymptomatic individuals would improve with the increasing number of testing. In that sense, the fraction of tested individuals among the population should be related to the ratio of reported infections to the total number of infections. This leads to the following expression

$$\begin{aligned}
\frac{I_t}{I_t^*} &= \exp(-k\rho_t) \\
\delta_t &= 1 - \exp(-k\rho_t).
\end{aligned} \tag{7}$$

Here  $\rho_t$  is the fraction of tests with positive outcomes among all tests. With the increasing number of testing on the population this fraction is expected to be low and therefore  $\delta_t$  approaches to 1. On the other hand, if testing is concentrated only on symptomatic individuals then this fraction is close to 1 and  $\delta_t$  approaches to a lower bound, captured by the parameter  $\exp(-k)$  where the functional form admits for exponential decay. We display the evolution of the model parameters estimated using (6) and (7) in Figure 3

for selected countries. Compared to previous sections, countries including Brazil, Iran and Russia are excluded from the sample as these countries do not provide accurate information on testing at daily frequency.

[Insert Figure 3 about here]

As can be seen from the graphs in the first row of Figure 3, we observe a sizable fraction of the infected individuals that do not show symptoms for many countries at the beginning of the sample. While this fraction is smallest for the South Korea, starting from 15% at the beginning of the sample decreasing to 4% in June, it is largest for US starting from 50% of all infected individuals decreasing to 30% in June. For Italy and Turkey, the fraction is about 20% and it declines to about 10% in June. The temporary increases in the fraction of asymptomatic individuals at the beginning of the sample is due to the efforts of these countries to increase their testing capacity in April. In this case, the speed of increase in the fraction of positive outcomes falls behind the speed of increase in the number of tests leading to ‘spuriously’ low values of  $\delta_t$ . However, once the capacity is reached we observe a monotonically decreasing pattern in the course of  $\delta_t$  as expected.

The impact of the relatively sizable fraction of the asymptomatic individuals for US can be seen from the last column of Figure 3. While the pattern of the evolution of the parameters remains unaffected there are some level shifts in all rates which seem to be diminishing towards June. We also observe similar level shifts of parameters for other countries, albeit limited compared to US case.

These effects are further aggravated when we consider  $R_{0,t}$  which is the ratio of the infection rate over the rate of resolution. In this case, for US and Italy,  $R_{0,t}$  differs considerably from the earlier estimates computed using the reported numbers at the beginning of the sample. The parameter values converge as the cumulative figures mount and this seems to have a little effect after the first half of the samples. Therefore, under these assumptions, the  $R_{0,t}$  computed using official statistics reflects progressively more and more the actual stance of the pandemic.

## 5 Conclusion

The world is struggling heavily to mitigate the spread of COVID-19 pandemic, which so far has devastating effects both from humanitarian and economic point of view. Countries

have been imposing various measures to fight the pandemic ranging from partial curfew to full lockdown to lower the transmission of the pandemic. These measures supposedly pave the way for the normalization of economies and reopening policies which has started since the early June in many countries. Health systems with overloaded intensive care units lead to substantial variation in the number of recoveries as well as daily death tolls over the course of the pandemic. Additionally, many countries including South Korea and Iran start to experience a second wave of the pandemic after the easing of the first wave. Therefore, the parameters in the workhorse epidemiological SIRD model, and ultimately the key statistics of the pandemic, i.e. the reproduction rate, change over time due to the change in these structural parameters.

In this paper, we extend the SIRD model allowing for time varying structural parameters for timely and accurate measurement of the stance of the pandemic. Our modeling framework falls into the class of generalized autoregressive score models, where the parameters evolve deterministically according to an autoregressive process in the direction implied by the score function. Therefore, the resulting approach permits quite a flexible yet parsimonious and statistically coherent framework that can operate in data scarce environments easily due to low computational cost. We demonstrate the potential of the proposed model using daily data from seven countries ranging from US to South Korea that have distinct pandemic dynamics over the last 6 months.

Our results show that the proposed framework can nicely track the stance of the pandemic in real-time. For all countries, the infection rate has reduced considerably but at differential speed depending on the success in containing the pandemic. Our findings suggest that there is considerable fluctuation in recovery and mortality rates, which seems to get more stable towards June. For US, Russia and Brazil the reproduction rate is above the critical level of 1 implying that these countries are unable to contain the pandemic yet. Our findings confirm the observation that Iran and South Korea experience the second wave of the pandemic. We further extend the model for including the infected individuals that do not show symptoms and therefore are not diagnosed. This seems to have a sizable impact on the estimated level of reproduction rate at the onset of the sample but converge to similar levels with the earlier findings towards the end of the sample.

## References

- Acemoglu D, Chernozhukov V, Werning I, Whinston MD. 2020. A multi-risk SIR model with optimally targeted lockdown. Working Paper 27102, National Bureau of Economic Research.
- Allen LJS. 2008. *An Introduction to Stochastic Epidemic Models*. Berlin, Heidelberg: Springer Berlin Heidelberg, 81–130.
- Anastassopoulou C, Russo L, Tsakris A, Siettos C. 2020. Data-based analysis, modelling and forecasting of the covid-19 outbreak. *PloS one* **15**: e0230405.
- Chen CW, Lee S. 2016. Generalized poisson autoregressive models for time series of counts. *Computational Statistics & Data Analysis* **99**: 51 – 67.
- Creal D, Koopman SJ, Lucas A. 2013. Generalized autoregressive score models with applications. *Journal of Applied Econometrics* **28**: 777–795.
- Davis RA, Dunsmuir WTM, Streett SB. 2003. Observation-driven models for poisson counts. *Biometrika* **90**: 777–790.
- Ferland R, Latour A, Oraichi D. 2006. Integer-valued garch process. *Journal of Time Series Analysis* **27**: 923–942.
- Fernandez-Villaverde J, Jones CI. 2020. Estimating and simulating a sird model of covid-19 for many countries, states, and cities. Working Paper 27128, National Bureau of Economic Research.
- Fokianos K, Rahbek A, Tjstheim D. 2009. Poisson autoregression. *Journal of the American Statistical Association* **104**: 1430–1439.
- Greenhalgh S, Day T. 2017. Time-varying and state-dependent recovery rates in epidemiological models. *Infectious Disease Modelling* **2**: 419 – 430.
- Grewelle R, De Leo G. 2020. Estimating the global infection fatality rate of covid-19. *medRxiv* .  
URL <https://www.medrxiv.org/content/early/2020/05/18/2020.05.11.20098780>
- Hale T, Petherick A, Phillips T, Webster S. 2020. Variation in government responses to covid-19. *Blavatnik school of government working paper* **31**.
- Hortaçsu A, Liu J, Schwieg T. 2020. Estimating the fraction of unreported infections in epidemics with a known epicenter: an application to covid-19. Technical report, National Bureau of Economic Research.
- Kermack WO, McKendrick AG. 1927. A contribution to the mathematical theory of epidemics. *Proceedings of the royal society of london. Series A, Containing papers of a mathematical and physical character* **115**: 700–721.
- Koopman SJ, Lucas A, Scharth M. 2016. Predicting time-varying parameters with parameter-driven and observation-driven models. *Review of Economics and Statistics* **98**: 97–110.

- Kucharski AJ, Russell TW, Diamond C, Liu Y, Edmunds J, Funk S, Eggo RM, Sun F, Jit M, Munday JD, Davies N, Gimma A, [van Zandvoort] K, Gibbs H, Hellewell J, Jarvis CI, Clifford S, Quilty BJ, Bosse NI, Abbott S, Klepac P, Flasche S. 2020. Early dynamics of transmission and control of covid-19: a mathematical modelling study. *The Lancet Infectious Diseases* **20**: 553 – 558. ISSN 1473-3099.
- Li R, Pei S, Chen B, Song Y, Zhang T, Yang W, Shaman J. 2020. Substantial undocumented infection facilitates the rapid dissemination of novel coronavirus (sars-cov-2). *Science* **368**: 489–493.
- Lourenco J, Paton R, Ghafari M, Kraemer M, Thompson C, Simmonds P, Klennerman P, Gupta S. 2020. Fundamental principles of epidemic spread highlight the immediate need for large-scale serological surveys to assess the stage of the sars-cov-2 epidemic. *MedRxiv* .
- Manski CF, Molinari F. 2020. Estimating the covid-19 infection rate: Anatomy of an inference problem. *Journal of Econometrics* .
- Marioli FA, Bullano F, Kučinskas S, Rondón-Moreno C. 2020. Tracking r of covid-19: A new real-time estimation using the kalman filter. *medRxiv* .
- Read JM, Bridgen JR, Cummings DA, Ho A, Jewell CP. 2020. Novel coronavirus 2019-ncov: early estimation of epidemiological parameters and epidemic predictions .
- Rizoiu MA, Mishra S, Kong Q, Carman M, Xie L. 2018. Sir-hawkes: linking epidemic models and hawkes processes to model diffusions in finite populations. In *Proceedings of the 2018 World Wide Web Conference*. 419–428.
- Robert C, Casella G. 2013. *Monte Carlo statistical methods*. Springer Science & Business Media.
- Tan SX, Chen L. 2020. Real-time differential epidemic analysis and prediction for COVID-19 pandemic. *arXiv preprint arXiv:2004.06888* .
- Wu JT, Leung K, Leung GM. 2020. Nowcasting and forecasting the potential domestic and international spread of the 2019-ncov outbreak originating in wuhan, china: a modelling study. *The Lancet* **395**: 689–697.
- Xu X, Kypraios T, O'Neill PD. 2016. Bayesian non-parametric inference for stochastic epidemic models using gaussian processes. *Biostatistics* **17**: 619–633.
- Yan P. 2008. *Distribution Theory, Stochastic Processes and Infectious Disease Modelling*. Berlin, Heidelberg: Springer Berlin Heidelberg, 229–293.
- Yang Q, Yi C, Vajdi A, Cohnstaedt LW, Wu H, Guo X, Scoglio CM. 2020. Short-term forecasts and long-term mitigation evaluations for the covid-19 epidemic in hubei province, china. *medRxiv* .
- Zhang Y, You C, Cai Z, Sun J, Hu W, Zhou XH. 2020. Prediction of the covid-19 outbreak based on a realistic stochastic model. *medRxiv* .

## Tables and Figures

Table 1: The dataset

Country	Time span
Brazil	March 08 - June 12
Italy	March 29 - June 12
Iran	March 29 - June 12
S. Korea	Febru. 26 - June 12
Russia	March 09 - June 12
Turkey	March 22 - June 12
US	March 11 - June 12

*Note:* The data is obtained from GitHub, COVID-19 Data Repository by the Center for Systems Science and Engineering (CSSE) at Johns Hopkins University.

Table 2: Estimation results of SIRD model

	$\beta$	$\gamma$	$\nu$	$R_0$
Brazil	0.101 (0.003)	0.050 (0.003)	0.005 (0.001)	1.834 (0.103)
Italy	0.036 (0.003)	0.026 (0.001)	0.005 (0.000)	1.163 (0.102)
Iran	0.097 (0.003)	0.077 (0.002)	0.005 (0.000)	1.194 (0.045)
S. Korea	0.033 (0.004)	0.033 (0.003)	0.001 (0.000)	0.979 (0.141)
Russia	0.055 (0.003)	0.028 (0.001)	0.001 (0.000)	1.957 (0.118)
Turkey	0.053 (0.003)	0.044 (0.003)	0.001 (0.000)	1.163 (0.104)
US	0.032 (0.002)	0.008 (0.000)	0.002 (0.000)	3.130 (0.221)

*Note:* The table displays the estimation results of the model in (2). We display the posterior modes and posterior standard deviations (in parenthesis) of the corresponding parameter shown in the first row and for the country shown in the first column.

Table 3: Estimation results of TVP-SIRD model parameters

	Brazil	Italy	Iran	S. Korea	Russia	Turkey	US
$\alpha_0$	-0.94 (0.02)	-0.84 (0.03)	-0.18 (0.02)	-0.23 (0.02)	-1.05 (0.02)	-1.08 (0.03)	-0.72 (0.00)
$\alpha_1$	0.59 (0.00)	0.76 (0.02)	0.93 (0.02)	0.95 (0.01)	0.64 (0.00)	0.65 (0.00)	0.80 (0.01)
$\alpha_2$	1.24 (0.01)	1.73 (0.03)	0.89 (0.10)	0.80 (0.07)	1.21 (0.04)	1.61 (0.01)	1.75 (0.00)
$\phi_0$	-1.07 (0.05)	-1.34 (0.02)	-0.18 (0.02)	-0.34 (0.03)	-1.35 (0.05)	-1.07 (0.02)	-1.53 (0.05)
$\phi_1$	0.64 (0.01)	0.63 (0.00)	0.93 (0.01)	0.89 (0.01)	0.62 (0.01)	0.62 (0.01)	0.68 (0.01)
$\phi_2$	0.78 (0.04)	1.31 (0.11)	0.91 (0.04)	0.64 (0.11)	1.38 (0.21)	1.59 (0.01)	0.77 (0.04)
$\psi_0$	-1.63 (0.06)	-1.52 (0.09)	-0.12 (0.01)	-0.49 (0.05)	-1.79 (0.00)	-1.78 (0.00)	-1.56 (0.21)
$\psi_1$	0.71 (0.01)	0.73 (0.01)	0.98 (0.00)	0.93 (0.01)	0.75 (0.00)	0.75 (0.00)	0.76 (0.03)
$\psi_2$	1.38 (0.15)	1.12 (0.08)	1.10 (0.08)	0.62 (0.07)	1.83 (0.00)	1.76 (0.00)	1.17 (0.04)

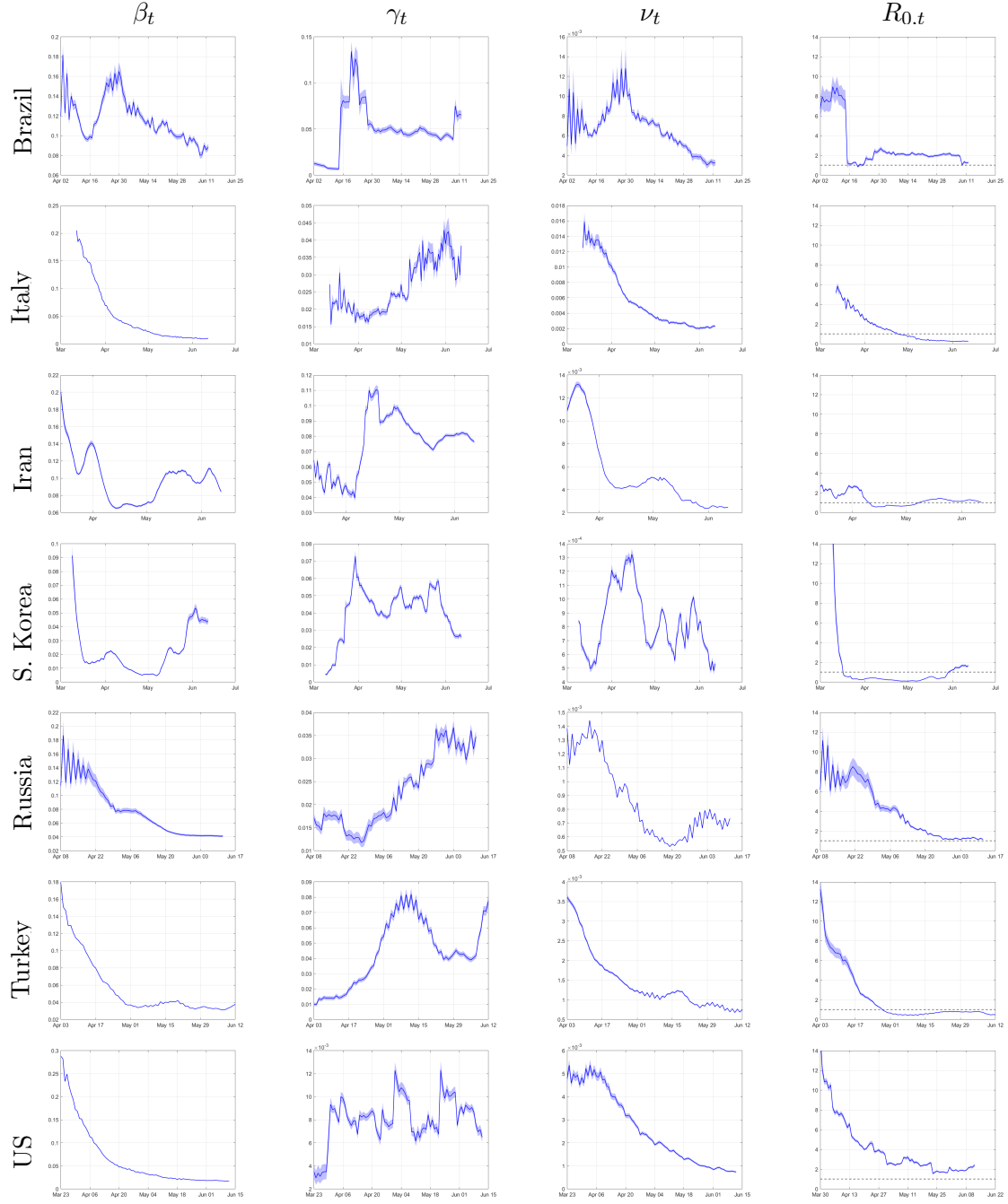
*Note:* The table displays the estimation results of the model in (4). We display the posterior modes and posterior standard deviations (in parenthesis) of the corresponding parameter shown in the first column and for the country shown in the first row.

Table 4: Relative RMSFEs of the competing models relative to TVP-SIRD model

		$h = 1$	$h = 2$	$h = 3$	$h = 4$	$h = 5$	$h = 6$	$h = 7$
Brazil	EW	2.19	1.97	1.81	1.65	1.49	1.37	1.26
	RW-10	1.63	1.49	1.39	1.31	1.22	1.15	1.07
	RW-20	1.88	1.71	1.57	1.44	1.31	1.22	1.12
	RW-30	2.03	1.83	1.68	1.54	1.40	1.30	1.19
Italy	EW	6.09	4.29	3.42	2.91	2.58	2.36	2.21
	RW-10	1.28	0.93	0.77	0.67	0.61	0.57	0.54
	RW-20	2.61	1.88	1.53	1.32	1.19	1.10	1.04
	RW-30	3.94	2.82	2.28	1.97	1.77	1.63	1.54
Iran	EW	3.50	2.53	2.09	1.85	1.72	1.64	1.58
	RW-10	2.22	1.65	1.39	1.26	1.17	1.11	1.06
	RW-20	3.02	2.20	1.82	1.63	1.51	1.43	1.38
	RW-30	3.40	2.46	2.04	1.81	1.68	1.59	1.54
S. Korea	EW	5.27	5.45	5.24	5.02	4.76	4.56	4.35
	RW-10	1.26	1.32	1.28	1.25	1.20	1.15	1.09
	RW-20	1.57	1.62	1.56	1.49	1.41	1.35	1.28
	RW-30	2.13	2.18	2.06	1.93	1.80	1.70	1.62
Russia	EW	4.76	2.95	2.31	1.98	1.79	1.66	1.57
	RW-10	1.51	0.99	0.82	0.73	0.69	0.66	0.65
	RW-20	2.68	1.71	1.37	1.21	1.11	1.06	1.02
	RW-30	3.63	2.29	1.82	1.59	1.45	1.37	1.31
Turkey	EW	5.52	3.39	2.62	2.23	2.01	1.86	1.77
	RW-10	2.22	1.42	1.14	1.00	0.92	0.87	0.83
	RW-20	3.95	2.46	1.92	1.65	1.49	1.39	1.33
	RW-30	5.01	3.09	2.40	2.06	1.86	1.73	1.65
US	EW	7.25	5.14	4.13	3.50	3.10	2.83	2.64
	RW-10	1.76	1.26	1.03	0.89	0.81	0.75	0.72
	RW-20	3.34	2.42	1.99	1.73	1.56	1.45	1.39
	RW-30	4.79	3.47	2.84	2.46	2.21	2.05	1.94

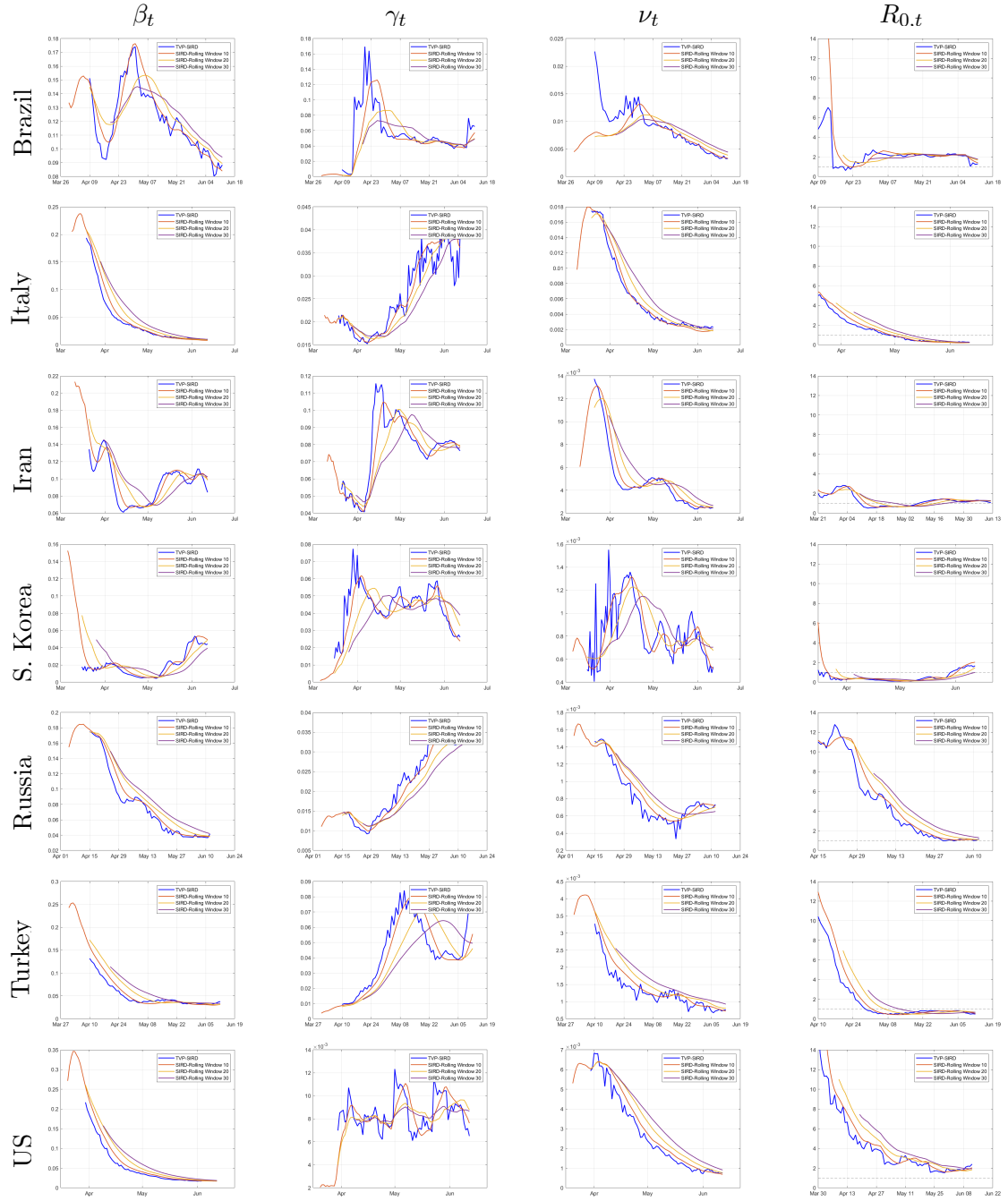
*Note:* The table displays the Root Mean Squared Forecast Errors (RMSFE) of the competing models relative to the TVP-SIRD model introduced in (4) for the country shown in the first column. EW stands for the Expanding Window. RW-M stands Rolling Window with  $M$  observations as the sample size for  $M = 10, 20, 30$ .

Figure 1: The evolution of  $\beta_t$ ,  $\gamma_t$ ,  $\nu_t$  and  $R_{0,t}$  estimated using TVP-SIRD model



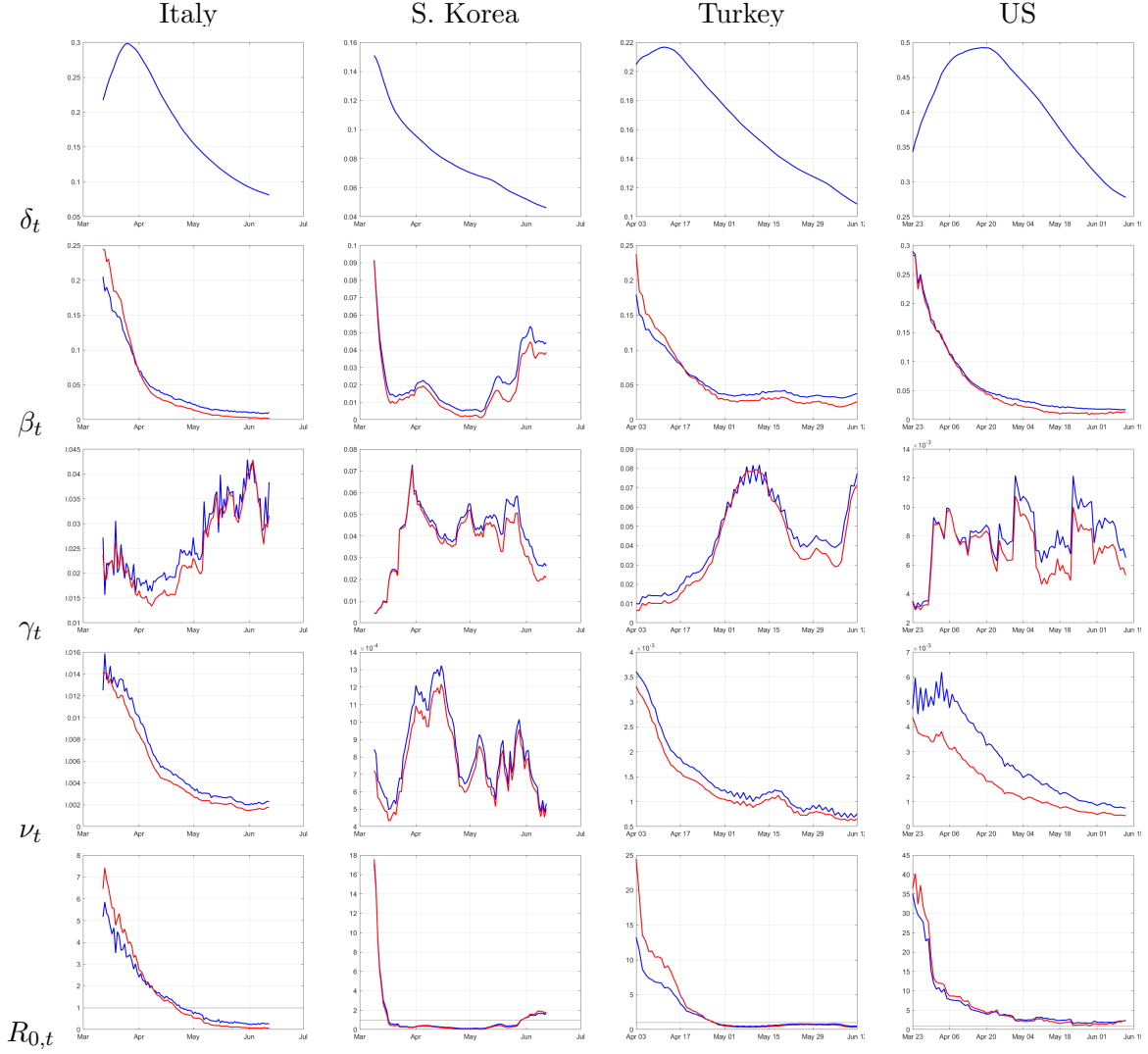
*Note:* The graphs show the evolution of the time varying parameters,  $\beta_t$ , the rate of infection,  $\gamma_t$ , the rate of recovery,  $\nu_t$ , the mortality rate and the resulting reproduction rate,  $R_{0,t}$  estimated using the TVP-SIRD model introduced in (4) for the countries shown in the first column.

Figure 2: Comparison of real-time estimates of parameters for competing models



*Note:* The graphs show the evolution of the time varying parameters in real-time, i.e. estimated using the sample up to the period  $t$  for the TVP-SIRD model (the blue line), estimated using the last  $M$  observations up to the period  $t$  for the SIRD model shown using the red, yellow and purple lines for  $M = 10, 20$  and  $30$  respectively. See Figure 1 for further details.

Figure 3: The evolution of  $\delta_t$ ,  $\beta_t$ ,  $\gamma_t$ ,  $\nu_t$  and  $R_{0,t}$  when asymptomatic infected individuals are also considered in the sample



*Note:* The graphs show the evolution of the time varying parameters,  $\delta_t$ , the fraction of asymptomatic cases in total cases,  $\beta_t$ , the rate of infection,  $\gamma_t$ , the rate of recovery,  $\nu_t$ , the mortality rate and the resulting reproduction rate,  $R_{0,t}$  estimated using the TVP-SIRD model introduced in (4) displayed with the blue line and the TVP-SIRD model that also takes the unreported cases into account introduced in (6) and (7) displayed with the red line.

## Appendix A Derivation of updating rules

Let  $f_1(\Delta C_t|\Omega_{t-1})$ ,  $f_2(\Delta R_t|\Omega_{t-1})$  and  $f_3(\Delta D_t|\Omega_{t-1})$  denote the conditional probability density functions for  $\Delta C_t$ ,  $\Delta R_t$  and  $\Delta D_t$  conditional on the information set at time period  $t-1$ ,  $\Omega_{t-1}$ , respectively. Assuming (conditional) independence among these variables, the conditional joint probability density function could be written as  $f(\Delta C_t, \Delta R_t, \Delta D_t|\Omega_{t-1}) = f_1(\Delta C_t|\Omega_{t-1})f_2(\Delta R_t|\Omega_{t-1})f_3(\Delta D_t|\Omega_{t-1})$ . We assume that these marginal distributions follow Poisson distribution with arrival rates specified in SIRD model in equation (2). Thus, the joint density is as follows,

$$f(\Delta C_t, \Delta R_t, \Delta D_t|\Omega_{t-1}) = \frac{\lambda_{1,t}^{\Delta C_t} \exp(-\lambda_{1,t})}{\Gamma(\Delta C_t+1)} \frac{\lambda_{2,t}^{\Delta R_t} \exp(-\lambda_{2,t})}{\Gamma(\Delta R_t+1)} \frac{\lambda_{3,t}^{\Delta D_t} \exp(-\lambda_{3,t})}{\Gamma(\Delta D_t+1)}, \quad (\text{A.1})$$

where  $\lambda_{1,t} = \beta_t \frac{S_{t-1}I_{t-1}}{N}$ ,  $\lambda_{2,t} = \gamma_t I_{t-1}$  and  $\lambda_{3,t} = \nu_t I_{t-1}$ . The score functions, denoted as  $\nabla_{1,t}$ ,  $\nabla_{2,t}$  and  $\nabla_{3,t}$ , can be written as

$$\begin{aligned} \nabla_{1,t} &= \left( \frac{\Delta C_t}{\lambda_{1,t}} - 1 \right) \left( \frac{I_{t-1}S_{t-1}}{N} \right) \\ \nabla_{2,t} &= \left( \frac{\Delta R_t}{\lambda_{2,t}} - 1 \right) I_{t-1} \\ \nabla_{3,t} &= \left( \frac{\Delta D_t}{\lambda_{3,t}} - 1 \right) I_{t-1} \end{aligned} \quad (\text{A.2})$$

We use the variance of the score functions for the scaling parameter. Variance of the score function for  $\nabla_{1,t}$ , for example, can be computed as

$$\begin{aligned} \text{Var}(\nabla_{1,t}|\Omega_{t-1}) &= E[\nabla_{1,t}\nabla_{1,t}'|\Omega_{t-1}] \\ &= E\left[\left(\frac{\Delta C_t}{\lambda_{1,t}} - 1\right)^2 \middle| \Omega_{t-1}\right] \left(\frac{I_{t-1}^2 S_{t-1}^2}{N^2}\right) \\ &= \frac{E[(\Delta C_t - \lambda_{1,t})^2|\Omega_{t-1}]}{\lambda_{1,t}^2} \left(\frac{I_{t-1}^2 S_{t-1}^2}{N^2}\right). \end{aligned} \quad (\text{A.3})$$

As  $E[(\Delta C_t - \lambda_{1,t})^2]$  refers to the variance of Poisson distributed random variable  $\Delta C_t$ , it is identical to  $\lambda_{1,t}$ . Hence, the resulting expression is,

$$\text{Var}(\nabla_{1,t}|\Omega_{t-1}) = \left( \frac{1}{\lambda_{1,t}} \right) \left( \frac{I_{t-1}^2 S_{t-1}^2}{N^2} \right) \quad (\text{A.4})$$

Similar computations lead to the variances of score functions for  $\Delta R_t$  and  $\Delta D_t$  as

$$\begin{aligned} \text{Var}(\nabla_{2,t}|\Omega_{t-1}) &= \frac{I_{t-1}^2}{\lambda_{2,t}} \\ \text{Var}(\nabla_{3,t}|\Omega_{t-1}) &= \frac{I_{t-1}^2}{\lambda_{3,t}} \end{aligned} \quad (\text{A.5})$$

Scaling (A.2) together with (A.4) and (A.5), the scaled score functions can be written as follows,

$$\begin{aligned} s_{1,t} &= (\Delta C_t - \lambda_{1,t}) \left( \frac{N}{I_{t-1} S_{t-1}} \right) \\ s_{2,t} &= \frac{\Delta R_t - \lambda_{2,t}}{I_{t-1}} \\ s_{3,t} &= \frac{\Delta D_t - \lambda_{3,t}}{I_{t-1}} \end{aligned} \quad (\text{A.6})$$

The final step includes the division of the scaled score functions by  $\beta_t$ ,  $\gamma_t$  and  $\nu_t$ , respectively, to obtain the scaled score function in terms of parameters with logarithmic transformations applying the chain rule. The resulting time evolution for  $\tilde{\beta}_t = \log(\beta_t)$ ,  $\tilde{\gamma}_t = \log(\gamma_t)$  and  $\tilde{\nu}_t = \log(\nu_t)$  is

$$\begin{aligned} \tilde{\beta}_t &= \alpha_0 + \alpha_1 \tilde{\beta}_{t-1} + \alpha_2 \left( \frac{\Delta C_{t-1} - \lambda_{1,t-1}}{\lambda_{1,t-1}} \right) \\ \tilde{\gamma}_t &= \phi_0 + \phi_1 \tilde{\gamma}_{t-1} + \phi_2 \left( \frac{\Delta R_{t-1} - \lambda_{2,t-1}}{\lambda_{2,t-1}} \right) \\ \tilde{\nu}_t &= \psi_0 + \psi_1 \tilde{\nu}_{t-1} + \psi_2 \left( \frac{\Delta D_{t-1} - \lambda_{3,t-1}}{\lambda_{3,t-1}} \right) \end{aligned} \quad (\text{A.7})$$

Combining (A.7) together with the SIRD equations, the final model becomes as follows

$$\begin{aligned} \Delta C_t | \Omega_{t-1} &\sim \text{Poisson}(\beta_t \frac{S_{t-1}}{N} I_{t-1}) \\ \Delta R_t | \Omega_{t-1} &\sim \text{Poisson}(\gamma_t I_{t-1}) \\ \Delta D_t | \Omega_{t-1} &\sim \text{Poisson}(\nu_t I_{t-1}) \\ \tilde{\beta}_t &= \alpha_0 + \alpha_1 \tilde{\beta}_{t-1} + \alpha_2 s_{1,t} \\ \tilde{\gamma}_t &= \phi_0 + \phi_1 \tilde{\gamma}_{t-1} + \phi_2 s_{2,t} \\ \tilde{\nu}_t &= \psi_0 + \psi_1 \tilde{\nu}_{t-1} + \psi_2 s_{3,t} \\ \Delta C_t = -\Delta S_t &= \Delta I_t + \Delta R_t + \Delta D_t \end{aligned} \quad (\text{A.8})$$

## Appendix B Implied Moments of the SIRD models

### B.1 SIRD Model

We assume that the initial values of states,  $S_0, I_0, R_0$  and  $D_0$  are known. For the sake of simplicity, we assume that  $S_t \approx N$ . We focus on the general form of equations as  $Y_t | \Omega_{t-1} \sim \text{Poisson}(\lambda I_{t-1})$  where  $\lambda = \beta, \gamma$  and  $\nu$  for  $Y_t = \Delta C_t, \Delta R_t$  and  $\Delta D_t$ , respectively. The conditional mean and the variance for the Poisson distributed variables are

$$\begin{aligned} E[Y_t | \Omega_{t-1}] &= \lambda I_{t-1} \\ \text{Var}(Y_t | \Omega_{t-1}) &= \lambda I_{t-1} \end{aligned} \tag{B.9}$$

The resulting process is stationary if the underlying process for  $I_t$  is stationary. This, in turn depends on the basic reproduction rate,  $R_0$ . To see this, we first start with  $\Delta I_t$  and use the fact that  $E[\Delta I_t] = E[\Delta C_t] - E[\Delta R_t] - E[\Delta D_t]$ . Therefore, the difference equation governing  $I_t$  takes the form of

$$\begin{aligned} I_t &= I_{t-1} + \Delta C_t - \Delta R_t - \Delta D_t \\ E[I_t | \Omega_{t-1}] &= I_{t-1} + \beta I_{t-1} - \gamma I_{t-1} - \nu I_{t-1} \\ &= (1 + \beta - \gamma - \nu) I_{t-1} \\ E[I_t] &= (1 + \beta(1 - R_0^{-1})) E[I_{t-1}] \end{aligned} \tag{B.10}$$

where the last equation uses the definition of the basic reproduction rate,  $R_0$ , as the ratio of the infection rate to the resolution rate. In case  $R_0$  exceeds unity, as  $\beta$  is positive, the process is explosive, i.e. the pandemic progress exponentially. On the other hand, if  $R_0$  falls below unity, the process becomes stationary. We can track down the process conditional on the starting value for  $I_0$ . Let  $\pi = (1 + \beta(1 - R_0^{-1}))$ .

$$E[I_t] = \pi^t I_0, \tag{B.11}$$

in case the initial condition is known, otherwise it is replaced by  $E[I_0]$ . For the variance we can use a similar recursion. We start with computing  $Var(I_t|\Omega_{t-1})$ .

$$\begin{aligned}
Var(I_t|\Omega_{t-1}) &= Var[\Delta C_t - \Delta R_t - \Delta D_t|I_{t-1}] \\
&= Var[\Delta C_t|I_{t-1}] + Var[\Delta R_t|I_{t-1}] + Var[\Delta D_t|I_{t-1}] \\
&= (\beta + \gamma + v)I_{t-1} \\
&= \beta(1 + R_0^{-1})I_{t-1}
\end{aligned} \tag{B.12}$$

By the law of total variance and using forward iteration, the unconditional variance can be computed as

$$\begin{aligned}
Var(I_t) &= \beta(1 + R_0^{-1})E[I_{t-1}] + \pi^2 Var(I_{t-1}) \\
&\vdots \\
&= \beta(1 + R_0^{-1})(\sum_{i=0}^{t-1} \pi^i) \pi^{t-1} E[I_0] + \pi^{2t} Var(I_0) \\
&= \beta(1 + R_0^{-1}) \frac{\pi^{t-1}(1-\pi^t)}{1-\pi} E[I_0] + \pi^{2t} Var(I_0)
\end{aligned} \tag{B.13}$$

In case the initial condition is known, the second term drops. Finally, we can use (B.11) and (B.13) for construction of the unconditional moments of  $Y_t$  as follows

$$\begin{aligned}
E[Y_t] &= \lambda E[I_t] \\
Var(Y_t) &= \lambda E[I_t] + \lambda^2 Var(I_t).
\end{aligned} \tag{B.14}$$

A common drawback of the models which involves variables assumed to follow Poisson distribution is that the conditional mean is assumed to be identical to the variance. However, as can be seen in above derivations, the spread of the random variable  $Y_t$  is greater than its expected value, i.e  $Var[Y_t] > E[Y_t]$ . Therefore, the model allows for overdispersion in the data.

## B.2 TVP-SIRD

As in the previous section, we focus on the general form of equations as  $Y_t|\Omega_{t-1} \sim \text{Poisson}(\lambda_t)$  where  $\lambda_t = \Psi_t I_{t-1}$  where  $\Psi_t = \beta_t, \gamma_t$  and  $\nu_t$  for  $Y_t = \Delta C_t, \Delta R_t$  and  $\Delta D_t$ , respectively. We consider  $W_t = \log(\lambda_t) = \log(\Psi_t) + \log(I_{t-1}) = \theta_t + K_{t-1}$  to insure positivity of the dynamic arrival rate. The time evolution of the model parameters is as follows

$$\theta_t = \alpha_0 + \alpha_1 \theta_{t-1} + \alpha_2 e_{t-1} \quad (\text{B.15})$$

where  $e_{t-1} = \frac{Y_{t-1} - \lambda_{t-1}}{\lambda_{t-1}}$ . Assuming stationarity for the evolution of the parameters, that would imply for  $\theta_t$  that

$$\theta_t = \frac{\alpha_0}{1-\alpha_1} + \sum_{i=1}^{t-1} \alpha_1^i \alpha_2 e_{t-i} = \gamma_0 + \sum_{i=1}^{\infty} \gamma_i e_{t-i} \quad (\text{B.16})$$

For  $e_t$ , given the initial conditions  $e_s = 0$  for  $s \leq 0$ , the mean of  $e_t$

$$\begin{aligned} E[e_t|\Omega_{t-1}] &= 0 \text{ for } s > 0, \text{ hence} \\ E[e_t] &= E[E[e_t|\Omega_{t-1}]] = 0 \end{aligned} \quad (\text{B.17})$$

Accordingly, the variance could be computed as,

$$E[e_t^2] = E[E[e_t^2|\lambda_t]] = E[\lambda_t^{-1}] \text{ for } s > 0. \quad (\text{B.18})$$

Moreover,  $\text{Cov}(e_t, e_s) = 0$  for  $t \neq s$ . This suggests that  $e_t$  series can be considered as i.i.d. innovations. Therefore, unconditional moments of  $\theta_t$  follows as

$$E[\theta_t] = \gamma_0 = \frac{\alpha_0}{1-\alpha_1}. \quad (\text{B.19})$$

and

$$\begin{aligned} \text{Var}(\theta_t) &= \sum_{i=1}^{\infty} \gamma_i^2 \text{Var}[e_{t-i}] \\ &= \sum_{i=1}^{\infty} \gamma_i^2 E[\lambda_{t-i}^{-1}] \\ \text{Cov}(\theta_t, \theta_{t-h}) &= \sum_{i=1}^{\infty} \gamma_i \gamma_{i+h} E[\lambda_{t-i}^{-1}] \end{aligned} \quad (\text{B.20})$$

Considering  $W_t = \theta_t + K_{t-1} = \gamma_0 + \sum_{i=1}^{\infty} \gamma_i e_{t-i} + K_{t-1}$

$$E[W_t] = \gamma_0 + E[K_{t-1}] \quad (\text{B.21})$$

and

$$\begin{aligned} Var(W_t) &= \sum_{i=1}^{\infty} \gamma_i^2 E[\lambda_{t-i}^{-1}] + Var(K_{t-1}) \\ Cov(W_t, W_{t-h}) &= \sum_{i=1}^{\infty} \gamma_i \gamma_{i+h} E[\lambda_{t-i}^{-1}] + Cov(K_{t-1}, K_{t-1-h}) \end{aligned} \quad (B.22)$$

where we use the i.i.d. property of the innovations. For deriving the expectations of the variables on the states of the pandemic, we use an approximation to Gaussian distribution and we can write

$$\begin{aligned} E[Y_t] &= E[E[Y_t|\lambda_t]] = E[\lambda_t] = E[\exp(W_t)] \\ &\approx \exp\left(\gamma_0 + E[K_{t-1}] + \frac{1}{2} \left(\sum_{i=1}^{\infty} \gamma_i^2 E[\lambda_{t-i}^{-1}] + Var(K_{t-1})\right)\right) \end{aligned} \quad (B.23)$$

see Davis et al. (2003). Moreover the unconditional variance of  $Y_t$  series follows from the law of total variance together with delta method as

$$\begin{aligned} Var(Y_t) &= E[\lambda_t] + Var(\lambda_t) \\ &\approx E[\lambda_t] + E[\lambda_t]^2 Var(W_t) \end{aligned} \quad (B.24)$$

Notice that  $\lambda_t$  is a linear function of  $I_{t-1}$ , and thus, the discussion provided on the properties of  $I_t$  in the previous section also applies here. An important distinction is that the process governing  $I_t$  in (B.10) is replaced with parameters that are time varying. Hence, score component of the model has a significant impact on the long run behavior of the model variables. We impose stationarity restrictions on the dynamic process governing  $\theta_t$ . Therefore, unconditional moments regarding to  $I_t$  can be derived similarly with  $\theta_t$  replaced with the unconditional mean and the variance of  $\theta_t$ .

Furthermore, let us consider the conditional variance  $Var(\theta_t|\Omega_{t-1}) = \alpha_2^2 \lambda_{t-1}^{-1}$ . Therefore, the time variation in the conditional variance of the data stems from both  $K_{t-1}$  and  $\theta_t$  and its evolution is characterized by the coefficients of lagged score variable. This provides considerably rich dynamics for capturing the evolution of the pandemic which is reflected as timely and prompt response of the parameters to the changes in the data, i.e. in the states of the pandemic which is reflected in Figure 1 and also Figure 2 where we consider the real-time performance of the models.